

Fall 2014

## **Examination of Tinnitus: Study of Synapses on Fusiform Cells in the Dorsal Cochlear Nucleus**

Stephanie BouAnak

*John Carroll University*, [sbouanak15@jcu.edu](mailto:sbouanak15@jcu.edu)

Follow this and additional works at: <https://collected.jcu.edu/honorspapers>

---

### **Recommended Citation**

BouAnak, Stephanie, "Examination of Tinnitus: Study of Synapses on Fusiform Cells in the Dorsal Cochlear Nucleus" (2014). *Senior Honors Projects*. 58.

<https://collected.jcu.edu/honorspapers/58>

This Honors Paper/Project is brought to you for free and open access by the Honor's Program at Carroll Collected. It has been accepted for inclusion in Senior Honors Projects by an authorized administrator of Carroll Collected. For more information, please contact [mchercourt@jcu.edu](mailto:mchercourt@jcu.edu).

**Examination of Tinnitus:**

**Study of Synapses on Fusiform Cells in the Dorsal Cochlear Nucleus**

Stephanie Bou-Anak and Dr. James Kaltenbach

John Carroll University- Cleveland Clinic

PS497N

Fall 2014

### **Abstract**

The dorsal cochlear nucleus (DCN) is a multimodal processing station found at the junction of the auditory nerve and brainstem medulla. Tinnitus-induced neuronal hyperactivity has been observed in the DCN and, thus, suggested to be the lowest region of the auditory nerve with such hyperactivity. The main integrative units of the DCN are the fusiform cells, receiving and processing inputs from auditory sources before transmitting information to higher auditory pathways. Neural hyperactivity is induced in fusiform cells of the DCN following intense sound exposure. Researchers suggest that fusiform cells may be implicated as major generators of noise-induced tinnitus. Despite previous research in describing fusiform cells and pharmacological identity of their synaptic inputs, information on their three-dimensional organization and ultrastructure is incomplete. This information is fundamental for the understanding of the normal characteristics of synapses on fusiform cells, synaptic plasticity and remodeling in hearing disorders, such as tinnitus. In this research study, serial block face scanning electron microscopy (SBFSEM) was used, followed by 3D reconstructions to quantitatively characterize and analyze the synaptic features on DCN fusiform cells. The results illustrate dense distribution of synapses and mitochondria on apical dendrites of fusiform cells.

## Introduction

Tinnitus is a condition characterized by the conscious perception of sound in the absence of actual sound or noise. Tinnitus caused by noise exposure is most often described as a ringing noise in one or both ears or even the head. While tinnitus is most prevalent in individuals older than 60 years of age, chronic tinnitus can develop at any age. In the United States, 12.5% of 6-12 year olds have developed elevated hearing thresholds in their audiograms caused by noise exposure from recreational sound (Niskar et al., 2001). Additionally, animal research has shown that noise exposure at a young age contributes to early onset of hearing loss and increased peripheral destruction of afferent neurons in exposed animals compared to unexposed animals (Kujawa and Liberman, 2006).

Researchers suggest that tinnitus is associated with some degree of hearing impairment. In fact, many tinnitus patients present dead cochlear regions (Weisz et al., 2006), threshold elevations compared to controls (Roberts et al., 2008) or outer hair cell damage (Job et al., 2007); all indications of hearing impairment. The most commonly studied pattern of hearing impairment in animal models on tinnitus involves elevated thresholds to high frequency sound (Roberts et al., 2010).

Although many studies have illustrated a central rather than peripheral origin to tinnitus, researchers lack concrete evidence about the initial region of the central auditory pathway leading to tinnitus. However, there is a growing body of evidence that tinnitus caused by noise exposure may be linked to a condition of hyperactivity of fusiform cells in the dorsal cochlear nucleus (DCN).

The DCN is a multimodal processing station found at the junction of the auditory nerve and brainstem medulla (Shore, 2005). This nucleus is composed of three layers: an outer

molecular layer, a middle fusiform cell layer and an inner polymorph layer (Osen and Mugnaini, 1981). Tinnitus-induced neuronal hyperactivity has been observed in the DCN and, thus, suggested to be the lowest region of the auditory nerve with such hyperactivity. The DCN is implicated in many auditory functions and connected with other auditory and non-auditory structures. For instance, the DCN is directly innervated by the auditory nerve. Cochlear injury caused by tinnitus-inducing agents may increase susceptibility of the auditory nerve to alterations of peripheral input, which, in turn, lead to the condition of hyperactivity observed in the DCN. Additionally, the DCN relays its information to higher order auditory centers and, in part, may contribute to increased activity at higher levels of the auditory pathway (Kaltenbach et al., 2007).

The main integrative units of the DCN are the fusiform cells which consist of apical dendrites protruding into the molecular layer of the DCN (Brawer et al., 1974). Neural hyperactivity is induced in fusiform cells of the DCN following intense sound exposure. Researchers suggest that fusiform cells may be implicated as major generators of noise-induced tinnitus (Manzoor et al., 2013).

Cells with the characteristics of fusiform cells show higher levels of hyperactivity in sound exposed animals than in unexposed controls (Brozoski et al., 2002). Ultrastructural and immunohistochemical research indicate that fusiform apical dendrites receive excitatory inputs from parallel fibers and inhibitory inputs from midbrain auditory nuclei and neighboring cartwheel and stellate cells (Rubio and Wenthold, 1999).

On the other hand, the cell body receives inhibitory inputs from nearby cartwheel cells, vertical cells, ventral cochlear nucleus, and midbrain auditory nuclei (Zhang and Oertel, 1994). The apical dendrites of fusiform cells can receive excitatory inputs from the auditory nerve to their spine and shaft terminals (Smith and Rhode, 1985) and some inhibitory inputs from vertical

cells and other sources (Voigt and Young, 1982). Previous studies have suggested that fusiform cell activity may be modulated by the activation of parallel fibers in normal hearing animals. The modulation is set up with a temporary excitation period of the fibers followed by a prolonged period of inhibition. This mechanism may reflect direct excitatory inputs to fusiform cells and indirect inhibitory inputs to fusiform cells via the cartwheel cell system (Manzoor et al., 2013).

Although the physiology and anatomy of fusiform cells have been described exclusively on the basis of two-dimensional imaging, there remain unexplored issues about spatial mapping of synapses on soma and dendritic spines and 3D characteristics of synaptic features. These include information on the three dimensional organization and ultra-structure of synapses on these cells, spine and terminal volumes, number of synapses and their active zones. A complete understanding of the synapses on the fusiform cells and how they are altered by noise may serve to advance research development on effective treatments for tinnitus.

The focus of the current study is to map and analyze the synaptic inputs to the soma and dendritic spines as well as characterize the factors contributing to inhibitory and excitatory inputs to fusiform cells. It is hypothesized that noise exposure causes tinnitus-related hyperactivity in the DCN by inducing changes in the physical characteristics of synapses on fusiform cells.

## **Material and Methods**

### **Animal Subjects**

Two control animals and two exposed animals used in the research were adult (80-82 days of age) male Syrian golden hamsters. The animals were obtained from Charles River Laboratories (Wilmington, Massachusetts) and retained in an animal vivarium on a 12 hr:12 hr light/dark cycle for 16-20 days before research use. The protocols implemented in the research were approved by the Institutional Animal Care and Use Committee (IACUC). The animal care

protocol implemented in the research was in accordance with the NIH Guidelines for the Care and Use of Animals in Research. Animals were divided into two groups with one group serving as a control and the other group exposed to intense sound.

### **Sound Exposure**

Exposed animals were placed in a sound attenuation booth inside of a cylindrical acrylic chamber (14 in X 18 in). The chamber was subdivided into 4 compartments; allowing the exposure of up to four animals simultaneously. The exposed sound was introduced through a 6 inch diameter Beyma CP-25 loudspeaker (Island Park, New York) mounted on the lid of the chamber. The exposed sound was set to 10 kHz pure tone with an intensity level adjusted to 115 dB Sound Pressure Level (SPL)  $\pm$  6 dB SPL. The sound exposure was maintained for a 4 hour period. At the end of the sound exposure, animals were tagged subcutaneously with an identification chip and returned to the vivarium for 16-20 days prior to research use.

### **Brain Tissue Fixation**

Following the 16-20 days post exposure recovery time, sound-exposed and age-matched controls were anesthetized using intramuscular injection of ketamine/xylazine (117 mg/kg – 18 mg/kg) and then perfused transcardially with 500 mL of 4% paraformaldehyde, 2% glutaraldehyde and 0.1 M sodium cacodylate. A tracheotomy and craniotomy were performed on each group of animals, and the left DCN was exposed. The brains were post-fixed in the same fixative for 24 hours. The fixed brains were trimmed under a light microscope to a block of brainstem tissue that contained the left DCN, medulla, pons and left inferior colliculus. The inclusion of these structures helped to localize the DCN after staining. The tissues were heavy metal-stained in 0.1% tannic acid for 60 minutes followed by ferrocyanide-reduced 2% osmium tetroxide for 60 minutes and 1% thiocarbohydrazide solution at 60°C for 30 minutes. The tissues

were washed in an alternating pattern with water or cacodylate solutions. The tissues were dehydrated in increasing concentrations of ethanol, then in 100% acetone. The tissues were embedded first in 50:50 mixtures of acetone and EPON (liquid bisphenol A based epoxy resin with n-butyl glycidyl ether) mixture overnight at room temperature, then in fresh 100% EPON in a mold for 48 hours at 60°C after being vacuumed.

### **Block Preparation**

The embedded tissue blocks were placed under a dissecting microscope with the dorsal surface of the DCN facing upwards. The blocks were cut with a razor blade in the transverse plane of the brain half-way between the rostral and caudal borders of the DCN. The blocks were placed inside in the microscope column and examined at 200X to confirm the orientation of the DCN. The region of interest was a rectangular area spanning the three layers of the DCN.

In order to obtain a better view of the region of interest, the blocks were removed from the microscope and further trimmed into a cube that encompassed the region of interest. The final trimmed blocks measured approximately 0.5 mm x 0.5 mm.

### **Slicing and Image Acquisition**

In order to examine the synapses of fusiform cells and study the effects of sound exposure on neural hyperactivity in the DCN, serial block face scanning electron microscopy (SBFSEM, Zeiss, Goettingen, Germany) was used, followed by 3D reconstructions to quantitatively characterize and analyze the synaptic features on DCN fusiform cells.

The final trimmed blocks were placed inside a Zeiss Sigma VP scanning electron microscope (Zeiss, Goettingen, Germany) equipped with a Gatan 3View stage/knife system (Gatan Inc., United States). The blocks were placed on the microtome stage with the transverse face of the DCN facing upwards. Serial sections of the blocks were cut at a thickness of 78-80

nm. The magnification of the microscope was set at 4000X and the electron beam at 2.0 kV using an aperture of 1.0  $\mu\text{s}/\text{voxel}$ . Images were captured per section sequentially in six adjacent but overlapping square fields, each measuring 78-80  $\mu\text{m}/\text{side}$ . The overlapping fields spanned the molecular, fusiform cell, and outermost part of the DCN. The six fields were imaged in a total of 550-650 sections. The final result was a set of six image stacks that spanned 225-240  $\mu\text{m}$  of DCN thickness.

### **Segmentation**

After image acquisition, the six stacks were stitched together using Fiji/ImageJ TrakEM (National Institutes of Health, United States) software into a montage that measured approximately 160 x 240  $\mu\text{m}$ . The outlines of fusiform cells and their dendrites and inputting synapses were traced and color-coded. In order to obtain a better understanding of the synaptic spatial distribution over the different compartments of the cell, the visible synaptic endings were traced over the somal surface. The visible synaptic endings were characterized by vesicle populations either close to the contact with the somal surface or distributed throughout the terminal. Dendrites and their spines, as well as pre-synaptic terminals impinging on the spines, were traced. The traced spines were qualitatively analyzed using Fiji/ImageJ TrackEM to discern whether each spine was contacted by more than one pre-synaptic terminal.

### **3D-Reconstruction**

Following segmentation, 3D imaging reconstruction of each neuron was performed by merging the traced structures along the Z-axis of the image stack utilizing TrakEM software. For control subjects, two neurons were obtained from the first animal and three neurons from the second animal. For exposed subjects, two neurons were obtained from one animal.

## **Data Analysis**

In order to quantify synaptic terminals on the fusiform cell soma, each terminal in the reconstructed image was individually identified with an identification number. Each terminal was isolated from the most distal point of the axon in which there was a clear distinction between axon and terminal. Terminal volumes were computed using TrakEM software. The measured volumes in a single fusiform cell were averaged in order to yield a group mean for each structure of interest. In order to test the significance of the mean data, ANOVA software (XLSTAT, United States) was used at a significance level of  $p \leq 0.05$ . The number of apical dendritic shaft terminal volumes and mitochondria of apical axo-dendritic synapses of the fusiform cells in the DCN were used to analyze the difference between control and exposed animals.

## **Results**

Fusiform cell FC3 from a control animal will be considered as a representative control fusiform cell. Fusiform cell FC4 from an exposed animal will be considered a representative exposed fusiform cell. The cells obtained from the animals were analyzed based on cell morphology, total number of synaptic inputs to fusiform cell apical dendrite, apical dendritic shaft terminal volumes, and mitochondria of apical axo-dendritic synapses. The apical dendrites of these cells were the focus of the study due to their higher terminal volumes and implications in neuronal hyperactivity.

### **Fusiform Cell Morphologies**

Fusiform cells FC3 and FC4, obtained from a control animal and an exposed animal respectively, were analyzed and characterized as two of the largest cells in the fusiform cell layer of the DCN with a one-axis elongation, as well as an extended apical dendrite (Figure 1A, B, Figure 2A, B).

### ***Control Animals***

The soma maximal diameter for fusiform cell FC3 was 24.37  $\mu\text{m}$  (Figure 3A). The apical dendrite consisted of primary branches that divided into secondary and tertiary branches. Apical dendrites contained spines that were densely populated on the secondary and tertiary apical dendritic branches. Fewer spines were noted on the primary apical dendritic branches. FC3 consisted of a round and centrally-located nucleus.

### ***Exposed Animals***

The soma maximal diameter for fusiform cell FC4 was approximately 18.07  $\mu\text{m}$  (Figure 3B). The apical dendrite consisted of primary branches that divided into secondary and tertiary branches. The apical dendrite contained spines that were densely populated on the secondary and tertiary apical dendritic branches. Fewer spines were noted on the primary apical dendritic branches. FC4 consisted of a round and centrally-located nucleus.

### **Total Number of Synaptic Inputs to Fusiform Cells**

A synaptic terminal was recognized by clearly established contacts with the soma and/or dendrites and distinguishing morphological characteristics from other elements, such as glial cells and neuropils (Figure 4 A, B).

### ***Control Animals***

The total number of synaptic terminals in control animals is exemplified by fusiform cell FC3 due to its symmetric distribution of dendritic branches in the apical dendrite. FC3 received a total of 370 terminals, of which 312 were noted on the apical dendrite. The apical dendrite contained 126 synaptic inputs on spines and 186 inputs on shafts.

### ***Exposed Animals***

The total number of synaptic terminals in exposed animals is exemplified by fusiform cell FC4 due to its symmetric distribution of dendritic branches in the apical dendrite. The synaptic inputs to FC4 are based upon terminals on the soma and the apical dendrite. FC4 received 140 terminals on the soma and 347 terminals on the apical dendrite. The apical dendrite contained 162 synaptic inputs on spines and 185 inputs on shafts.

### **Axo-Dendritic Synapses**

Synaptic terminals were traced and analyzed on the shafts and spines of the apical dendrites of fusiform cell FC3 of the control animal and fusiform cell FC4 of the exposed animal.

### ***Control Animals***

A total of 312 synapses, including shaft terminals and spine, were traced on the apical dendrite of FC3. Of the total synapses, 186 (60%) were shaft terminals and 126 (40%) were spine terminals. The mean volume of shaft terminals on the apical dendrite of FC3 was  $3.09 \pm 4.0 \mu\text{m}^3$  (mean  $\pm$  S.D.) with minimal variation across terminals in FC3. These findings suggest that the inputs are somewhat identical across terminals of a fusiform cell.

### ***Exposed Animals***

A total of 347 synapses, including shaft terminals and spine, were traced on the apical dendrite of FC4. Of the total synapses, 185 (53%) were shaft terminals and 162 (47%) were spine terminals. The mean volume of shaft terminals on the apical dendrite of FC4 was  $2.14 \pm 3.31 \mu\text{m}^3$  (mean  $\pm$  S.D.) with minimal variation across terminals in FC4. These findings also suggest that the inputs are somewhat identical across terminals of a fusiform cell.

### **Mitochondria of Axo-Dendritic Synapses**

Mitochondria on axo-dendritic shaft terminals were recognized as dark structures within the terminal. The mitochondria may be characterized as round, oval, or complex-shaped (Figure 4 A, B).

#### ***Control Animals***

Mitochondria on axo-dendritic shaft terminals were counted and analyzed on 50 of the 99 shaft terminals on an apical dendrite of the fusiform cell FC3 (Figure 4A). Of the 50 shaft terminals, the mean mitochondrial count was calculated to be  $3.9 \pm 3.1$  (mean  $\pm$  S.D.).

#### ***Exposed Animals***

Mitochondria on axo-dendritic shaft terminals were counted and analyzed on 50 of the 185 shaft terminals on the apical dendrite of the fusiform cell FC4 (Figure 4B). Of the 50 shaft terminals, the mean mitochondrial count was calculated to be  $5.22 \pm 9.9$  (mean  $\pm$  S.D.).

### **Discussion**

The findings of a quantitative morphometric analysis and mapping of an array of synaptic features on DCN fusiform cells (such as, the numbers, volumes and ultrastructure of synaptic endings and dendritic spines) have been depicted. The purpose of this analysis was to establish a foundation for future studies focusing on determining how variations of input and different pathological states impact the synaptic features of fusiform cells. Specifically, this project may serve as a foundational study in analyzing the connection between tinnitus and neuronal hyperactivity in the DCN.

### **Changes in Cell Size as a Basis for Neuronal Hyperactivity**

Cell size reduction may be associated with neuronal degeneration and deafness, such as tinnitus. Reduction of cell size has been observed in brainstem auditory nuclei of humans with

adult-onset deafness (Moller et al., 2007). A similar study has been performed on a different type of cell in the DCN showing soma reduction after exposure to loud noise (Asako et al., 2005). That study reported, a reduction in soma area of DCN tuberculoventral cells in animals after two weeks following cochlear ablation.

Reduction in cell size has been suggested to decrease the duration and rate of action potentials. Evidence suggests that neurons with shorter durations would generally have weaker synaptic strengths and weaker neurotransmitter release. Therefore, if cell shrinkage involves fusiform cells with inhibitory synapses, the effect may be a reduction in the strength of inhibition of DCN neurons and thus an increase in excitatory activity or hyperactivity (Moller et al., 2007).

Cell reduction is noted in this study; although the findings are based on a representative sample of neurons. Fusiform cell FC3 was reported to have a maximal soma diameter of 24.37  $\mu\text{m}$  while fusiform cell FC4 of the exposed animal was reported to have a maximal soma diameter of 18.07  $\mu\text{m}$ . Thus, FC4 of the exposed animal was observed to have a 25% reduction in soma diameter from FC3 of the control animal. The findings of this study suggest a correlation with the published data discussed above. Therefore, soma reduction in fusiform cells may suggest reduced inhibitory synapses and provide a basis for neuronal hyperactivity and tinnitus.

### **Differences in Synapse Size**

Volumetric measures have detected a slight difference in synapse size between FC3 and FC4. FC3 was reported to have a mean apical dendritic shaft terminal volume of was  $3.09 \pm 4.0 \mu\text{m}^3$ , and FC4 was reported to have a mean apical dendritic shaft terminal volume of  $2.14 \pm 3.31 \mu\text{m}^3$ . Thus, FC4 of the exposed animal was observed to have a 31% reduction in apical dendritic shaft terminal volume from FC3 of the control animal. The decrease in terminal volume may be

associated with the reduction in inhibitory synapses and the decrease in the strength of neurotransmission due to neuronal hyperactivity.

### **Differences in Mitochondrial Density**

Mitochondria are significant structures in aerobic respiration, calcium ion homeostasis, and apoptosis. The activity and distribution of mitochondria are adaptable to physiological changes in the metabolic processes of the cell. In fact, the control of mitochondrial distribution plays an important role in the high metabolic demands of neurons due to their complex morphology (i.e., dendrites, axons, and synapses). Neuronal mitochondria are typically found in regions of intense energy consumption and high metabolic demands, such as synaptic terminals (Lee and Peng, 2008). Hyperactive neurons entail higher metabolic demands and, thus, are expected to contain a greater number of mitochondria than neurons with regular activity. In this study, fusiform cell FC4 of the exposed animal resulted in a higher mean number of mitochondria per dendrite ( $5.22 \pm 9.9$ ) than fusiform cell FC3 of the control animal ( $3.9 \pm 3.1$ ). Although the analysis involved one apical dendrite per cell for each group of animals, the data does support the hypothesis of mitochondrial density with neuronal hyperactivity and tinnitus (Khatri and Man, 2013). Therefore, the findings suggest that noise-induced tinnitus in the exposed animal resulted in neuronal modulation with increased mitochondrial density to compensate for the energy expenditure generated by neuronal hyperactivity.

### **Functional Significance and Relation to Tinnitus**

Evidence from clinical studies of patients with acoustic neuromas is consistent with implicating the DCN as a major site of tinnitus-related neuronal hyperactivity (Soussi and Otto, 1994). In that study, patients received brainstem auditory implants on the surface of the DCN followed by bilateral resection of the auditory nerves. The study reported that most patients

experienced no change in their tinnitus-associated symptoms upon the application of the implant. However, patients reported a decrease in perceived loudness or severity of their tinnitus-associated symptoms upon application of current by the implant to the DCN. Thus, the study suggests the modulatory effects of the DCN on tinnitus-related hyperactivity.

Tinnitus-related neuronal hyperactivity may be related to loss of inhibitory synapses and increase of excitatory synapses. Although this study did not focus on analyzing the types of synapses present in the cells, the excitation of synapses, characterized by having an increase in the number of active zones and post-synaptic densities, has been shown to play a role in the regulation of neuronal hyperactivity in the DCN. Furthermore, the increase in synaptic excitation may be attributed to the loss of inhibitory synapses due to a reduction in soma size and weaker neurotransmission.

The purpose of this study is not intended to implicate the DCN as the only structure attributed to tinnitus. However, the DCN is involved with the development, modulation and psychological phenomenon of tinnitus. Hyperactivity may occur at any level of the auditory pathway and result in the generation of tinnitus, as has been previously suggested (Moller et al., 2007). There are other brain structures that may be important in the development of tinnitus. Brain areas other than those in the midbrain and medulla may contribute to the behavioral and emotional aspects of tinnitus. However, the fact that the DCN is involved in many of the main features of hyperactivity, such as the generation and modulation of tinnitus, creates a compelling case for the analysis of the DCN. Future studies will be necessary to determine the extent to which the DCN participates in neuronal hyperactivity and the pathological outcome of tinnitus.

## References

- Asako, Mikiya, Avril G. Holt, Ronald D. Griffith, Eric D. Buras, and Richard A. Altschuler. "Deafness-related Decreases in Glycine-immunoreactive Labeling in the Rat Cochlear Nucleus." *Journal of Neuroscience Research* 81.1 (2005): 102-09. Web.
- Blackstad, T.W., Osen, K. K., & Mugnaini, E. (1984). Pyramidal neurones of the dorsal cochlear nucleus: a Golgi and computer reconstruction study in cat. *Neuroscience*, 13, 827–854.
- Brawer, J.R., Morest D.K., & Kane, E.C. (1974). The neuronal architecture of the cochlear nucleus of the cat. *Journal of Comparative Neurology*, 155:251-300.
- Brozoski, T.J., Bauer, C.A., & Caspary, D.M. (2002). Elevated fusiform cell activity in the dorsal cochlear nucleus of chinchillas with psychophysical evidence of tinnitus. *Journal of Neuroscience*, 22(6), 2383-2390.
- Fujino, K., & Oertel, D. (2003). Bidirectional synaptic plasticity in the cerebellum-like mammalian dorsal cochlear nucleus. *Proceedings of the National Academy of Sciences of the United States*, 100, 265–270.
- Job, A., Raynal, M., & Kossowski, M. (2007). Susceptibility to tinnitus revealed at 2 kHz range by bilateral lower DPOAEs in normal hearing subjects with noise exposure. *Audiology and Neurotology*, 12:137–144.
- Kaltenbach, J.A. (2007). The dorsal cochlear nucleus as a contributor to tinnitus: mechanisms underlying the induction of hyperactivity. *Progress in Brain Research*, 166:89–106.
- Khatri, N., & Man, H.Y. (2013). Synaptic activity and bioenergy homeostasis: Implications in brain trauma and neurodegenerative diseases. *Frontiers in Neurology*, 4, 199.
- Kujawa, S., & Liberman, M.C. (2006). Acceleration of age-related hearing loss by early noise exposure: evidence of a misspent youth. *Journal of Neuroscience*, 26(7):2115 –2123.

- Lee, C.W., & Peng, B.H. (2008). The function of mitochondria in presynaptic development at the neuromuscular junction. *Molecular Biology of the Cell*, 19:150-158.
- Manzoor, N. F., Gao, Y., Licari, F., & Kaltenbach, J.A. (2013). Comparison and contrast of noise-induced hyperactivity in the dorsal cochlear nucleus and inferior colliculus. *Hearing Research*, 295, 114-123.
- Moller, Aage R., Goran Hajak, Tobias Kleinjung, and Anthony Cacace.  
"Pathophysiology." *Tinnitus: Pathophysiology and Treatment*. By Berthold Langguth. Amsterdam: Elsevier, 2007. 95-100. Print.
- Mugnaini, E., Osen, K. K., Dahl, A. L., Friedrich, V. L. Jr., & Korte, G. (1980a). Fine structure of granule cells and related interneurons (termed Golgi cells) in the cochlear nuclear complex of cat, rat and mouse. *Journal of Neurocytology*, 9, 537–570.
- Niskar, A.S., Kieszak, S.M., Holmes, A.E., Esteban, E., & Rubin, C. (2001). Estimated prevalence of noise-induced hearing threshold shifts among children 6 to 19 years of age: the Third National Health and Nutrition Examination Survey, 1988–1994, United States. *Pediatrics*, 108: 40–43.
- Osen, K.K., & Mugnaini, E. (1981). Neuronal circuits in the dorsal cochlear nucleus. In: *Neuronal Mechanisms of Hearing*, edited by J. Syka and L. Aitken. *New York: Plenum*, 119-125.
- Roberts, L.E., Moffat, G., Baumann, M., Ward, L.M., & Bosnyak, D.J. (2008). Residual inhibition functions overlap tinnitus spectra and the region of auditory threshold shift. *Journal of the Association for Research in Otolaryngology*, 9:417– 435.

- Roberts, L.E., Eggermont J.J., Caspary D.M., Shore, S.E., Melcher, J.R., & Kaltenbach, J.A. (2010). Ringing ears: The neuroscience of tinnitus. *The Journal of Neuroscience*, 30:14972–14979.
- Rubio, M.E., & Wenthold, R.J. (1997). Glutamate receptors are selectively targeted to postsynaptic sites in neurons. *Neuron*, 18:939-950.
- Schikorski, T., & Stevens, C. F. (1997). Quantitative ultrastructural analysis of hippocampal excitatory synapses. *Journal of Neuroscience*, 17, 5858–5867.
- Shore, S.E. (2005). Multisensory integration in the dorsal cochlear nucleus: unit responses to acoustic and trigeminal ganglion stimulation. *European Journal of Neuroscience*, 21:3334-3348.
- Smith, P.H., & Rhode, W.S. (1985). Electron microscopic features of physiologically characterized, HRP-labeled fusiform cells in the cat dorsal cochlear nucleus. *Journal of Comparative Neurology*, 237:127-143.
- Soussi, T., & Otto, S.R. (1994). Effects of electrical brainstem stimulation on tinnitus. *Acta Otolaryngologica*, 114:135-140.
- Weisz, N., Hartmann, T., Dohrmann, K., Schlee, W., & Noreña, A. (2006). High-frequency tinnitus without hearing loss does not mean absence of deafferentation. *Hearing Research*, 222:108-114.
- Zhang, S., & Oertel, D. (1994). Neuronal circuits associated with the output of the dorsal cochlear nucleus through fusiform cells. *Journal of Neurophysiology*, 71:914-930.

## Figure Legends

### Figure 1. 3-D reconstruction of fusiform cells

- A:** 3D-reconstructions of the control fusiform cell FC3 cell somata (blue) and selected apical dendrites (green and blue) containing shaft terminals (light blue) and spines (yellow/brown).
- B:** 3D-reconstructions of the exposed fusiform cell FC4 cell somata (purple) and selected apical dendrites (red) containing shaft terminals (yellow) and spines (blue and green).

### Figure 2. 3-D reconstruction of apical dendrites

- A:** 3D-reconstructions of the control fusiform cell FC3 apical dendrite (blue).
- B:** 3D-reconstructions of the exposed fusiform cell FC4 apical dendrite (red).

### Figure 3. Morphology of fusiform cells

- A:** Transverse section through the control fusiform cell FC3 shown at maximum soma diameter. The diameter for FC3 was 24.37  $\mu\text{m}$ . The nucleus (N) and nucleolus (Nu) are shown.
- B:** Transverse section through the exposed fusiform cell FC4 shown at maximum soma diameter. The diameter for FC4 was 18.07  $\mu\text{m}$ . The nucleus (N) and nucleolus (Nu) are shown.

### Figure 4. Morphology of apical dendritic shaft terminals

- A:** Transverse section through a selected shaft terminal (T) on apical dendrite (turquoise) of the control fusiform cell FC3, containing mitochondria (M).
- B:** Transverse section through a selected shaft terminal (T) on apical dendrite (red) of the exposed fusiform cell FC4, containing mitochondria (M).

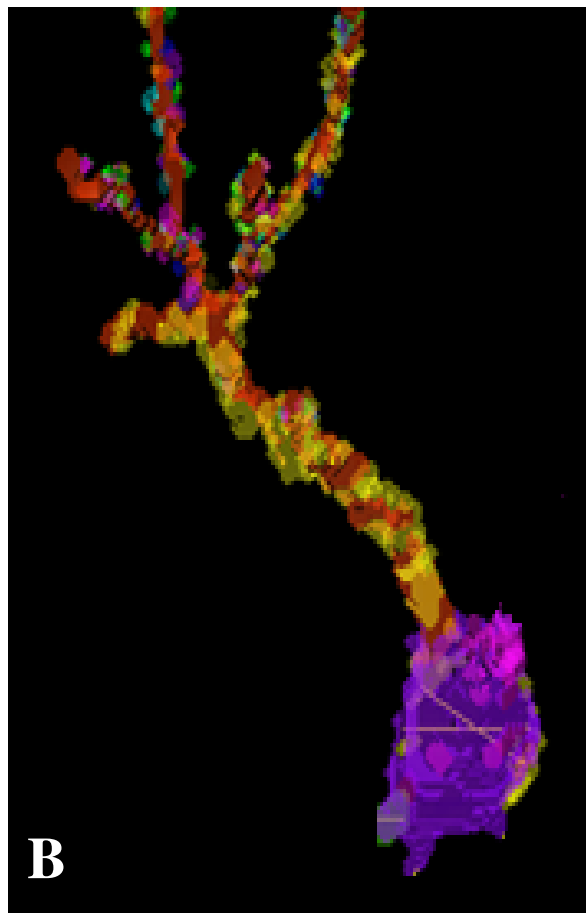
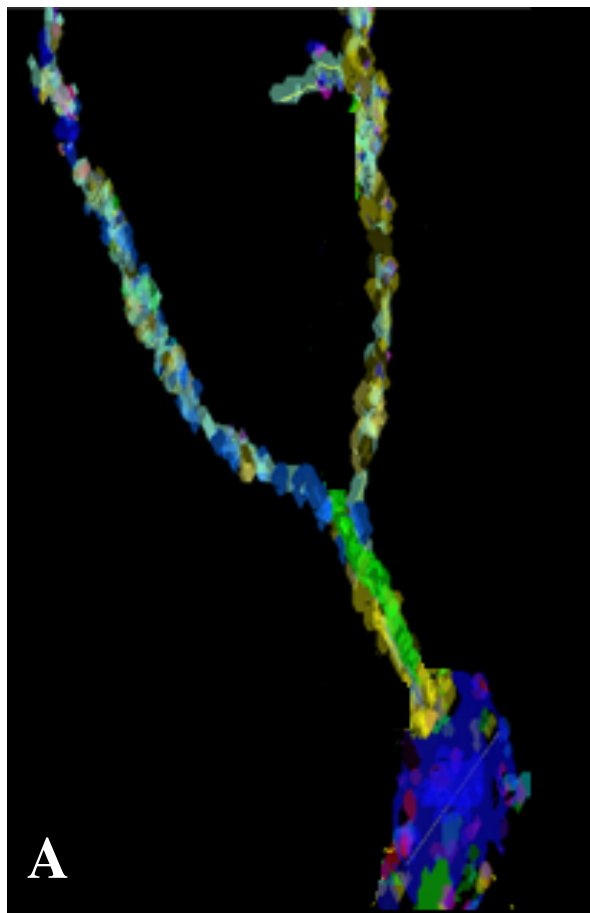


Figure 1

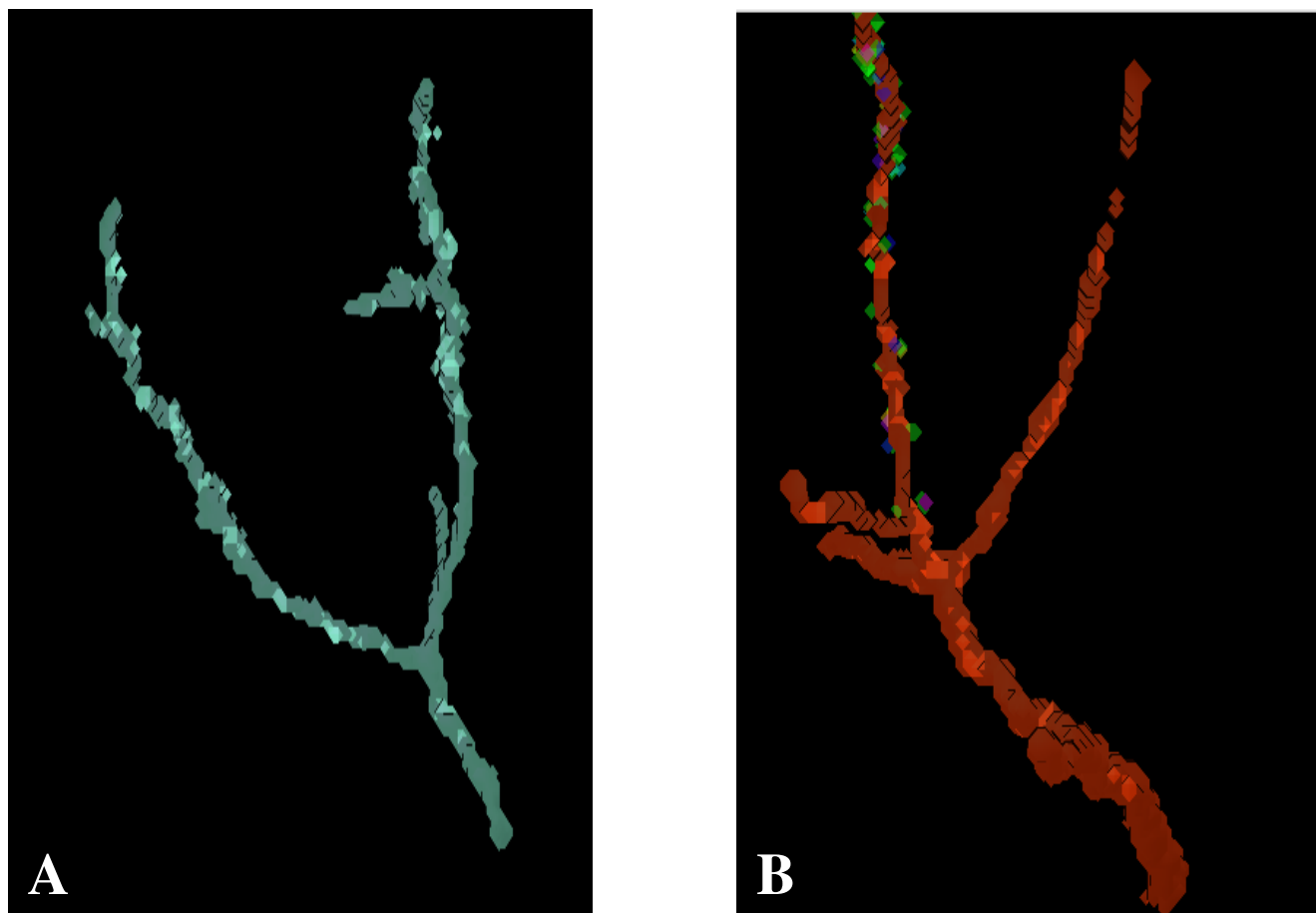


Figure 2

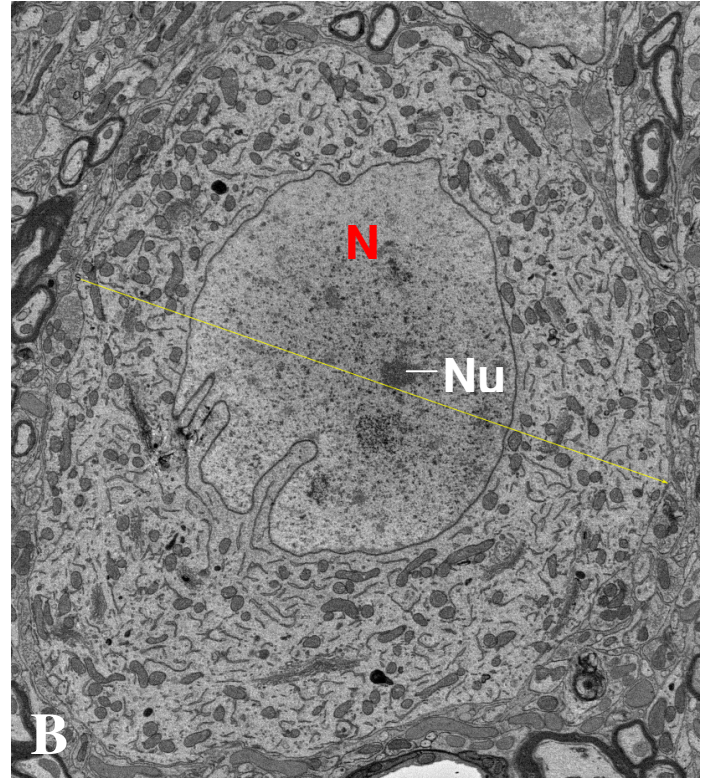
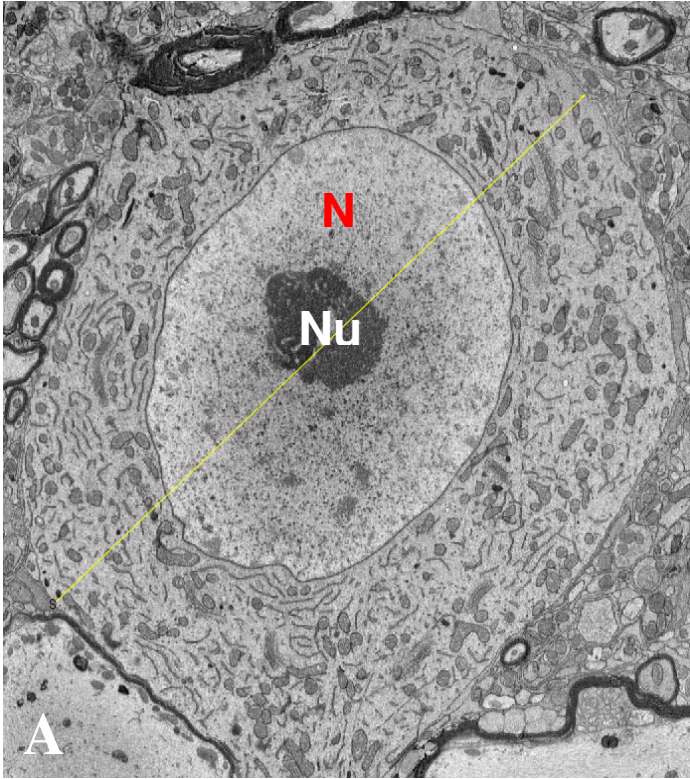


Figure 3

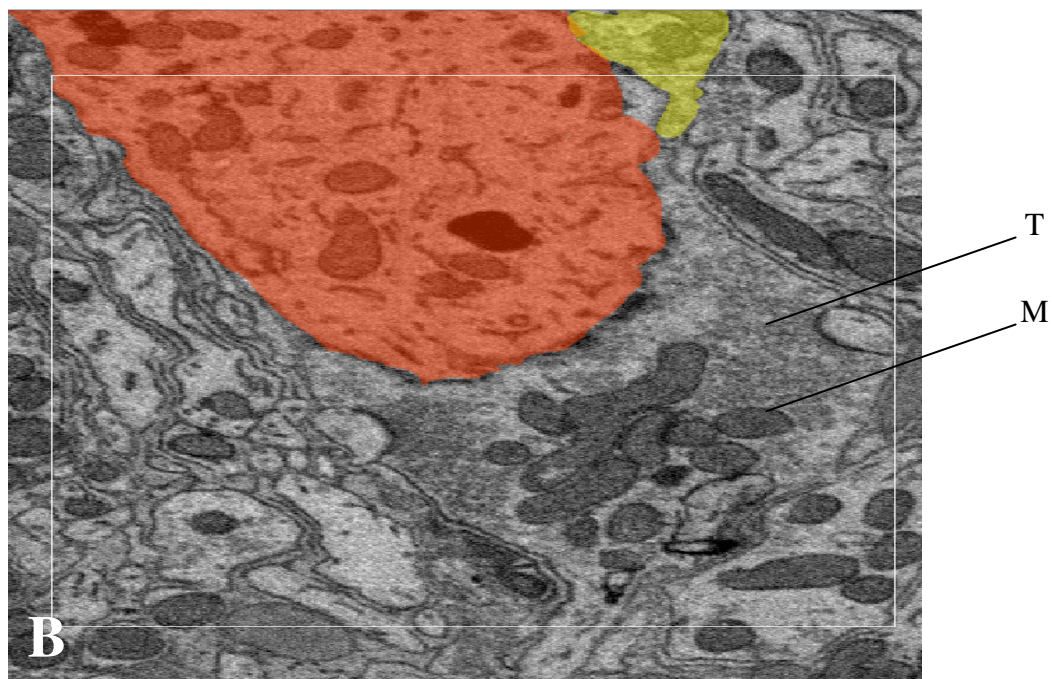
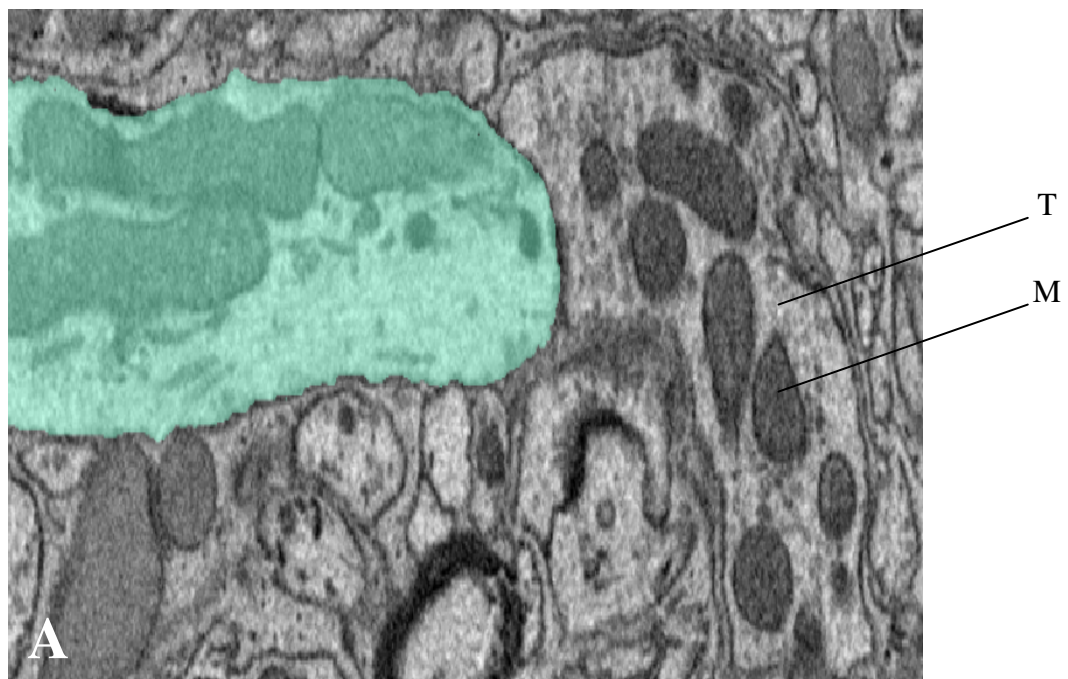


Figure 4